NUCLEIC ACID THERAPEUTICS
Volume 23, Number 4, 2013

DOI: 10.1089/nat.2013.0419

Fully Phosphorothioate-Modified CpG ODN with PolyG Motif Inhibits the Adhesion of B16 Melanoma Cells *In Vitro* and Tumorigenesis *In Vivo*

Xueju Wang,[1,2] Liying Wang,[1,2] Min Wan,[1] Xiuli Wu,[1] Yongli Yu,[3] and Liping Wang[2]

Adhesion to the extracellular matrix and endothelial lining of blood vessels is critical for tumor cells to grow at original or metastatic sites. Inhibition of tumor cell adhesion can be an antitumor strategy. Guanosine-rich (G-rich) oligodeoxynucleotides (ODNs) can inhibit the adhesion of certain tumor cells. However, no data exist on how inclusion of the CpG motif in the G-rich sequence influences tumor cell adhesion and subsequent tumorigenesis. In this study, *in vitro* and *in vivo* assays were used to evaluate how a panel of ODN-containing contiguous guanosines and the CpG motif influenced adhesion of B16 melanoma cells. The results showed that a self-designed ODN, named BW001, containing the polyG motif and a full phosphorothioate modification backbone could inhibit B16 melanoma cell adhesion on a culture plate or on a plate coated with various substances. *In vivo* data revealed that B16 melanoma cells co-administered with BW001 and intraperitoneally injected into mice formed fewer tumor colonies in peritoneal cavities. This effect was related to the polyG motif and the full phosphorothioate modification backbone and enhanced by the existence of the CpG motif. Additional *in vivo* data showed that survival of tumor-bearing mice in the BW001 group was significantly prolonged, subcutaneous melanoma developed much more slowly, and lung dissemination colonies formed much less often than in mice inoculated with B16 melanoma cells only. The effect was CpG motif-dependent. These results suggest that BW001 may exert an integrated antitumor effect.

Introduction

Adhesion of tumor cells or transformed cells to the extracellular matrix (ECM), especially adhesion to vessel endothelial cells or epithelial cells of secondary organs, significantly contributes to tumorigenesis at original or metastatic sites (Langley et al., 2007; Li et al. 2009; Damsky et al., 2011; Vaid et al., 2011). Inhibition of these adhesion processes has been considered a valuable approach for antitumor therapy (McGary et al., 2003; Braeuer et al., 2012; Wicklein 2012).

Both guanosine-rich (G-rich) oligodeoxynucleotides (ODNs) and CpG ODNs are a promising new type of therapeutic agent for malignant tumors. G-rich ODNs (GROs) can induce multiple antitumor effects such as stimulation of the immune system, inhibition of a tumor cell's proliferation or adhesion, and mediation of cell apoptosis (Bates et al, 2009). Similarly, CpG ODN also exhibits various antitumor effects such as inhibition of tumor growth in a mouse model by recognition of toll-like receptor 9 (TLR9) expressed in dendritic cells and B cells (Yang et al., 2009; Sommariva et al., 2011; Kim et al., 2012; Yan et al., 2012), and induction of tumor cell apoptosis or inhibition of tumor cell proliferation *in vitro* by reacting with TLR9 overexpressed in certain tumor strains (El Andaloussi et al., 2006; Zent et al., 2012). Among these effects, the tumor adhesion-inhibiting potential of ODN has been relatively rarely reported. Khaled et al. first reported that phosphorothioate (PS) ODN, with more than 4 contiguous guanosines, could inhibit cell adhesion *in vitro* (Khaled et al., 1996). Another research group also provided evidence that a contiguous 4-guanosine sequence in c-myelocytomatosis oncogene (c-myc) antisense phosphorothioate oligonucleotides could inhibit the growth of human lung cancer cells by possible involvement with cell adhesion inhibition (Saijo et al., 1997). However, there are still no detailed data on the effect of the inclusion of the CpG motif on the anti-adhesive potential of GRO.

In this study, we tested a series of self-designed ODNs with contiguous guanosine sequences and the CpG motif for their influence on the adhesion of melanoma cells. We found that candidate ODNs with a sequence containing more than 4 contiguous guanosines and full PS modification could inhibit

[1]Department of Molecular Biology, Norman Bethune College of Medicine, Jilin University, Changchun, China.
[2]Department of Pathology, China-Japan Union Hospital of Jilin University, Changchun, China.
[3]Department of Immunology, Norman Bethune College of Medicine, Jilin University, Changchun, China.

B16 melanoma cell adherence, spread, and proliferation in various *in vitro* and *ex vivo* assays. The anti-adhesive potential was not CpG motif-dependent. However, a series of *in vivo* experiments demonstrated that one of the above-mentioned candidate ODNs containing the CpG motif, named BW001, which has been proven to have strong effects against severe acute respiratory syndrome–coronavirus (Bao et al., 2006) and Coxsackie B3 virus (Cong et al., 2007), outshone other ODN candidates due to its tumorigenesis-inhibiting effects. These effects included decreasing tumor colony formation in the peritoneal cavity, prolonging the survival time of tumor-bearing mice, delaying the growth of subcutaneous tumors, and inhibiting lung dissemination of B16 cells. In summary, we are the first to report that PS ODN containing polyguanosine (polyG) and CpG motifs can inhibit tumor cell adhesion *in vitro* and tumorigenesis *in vivo*.

Materials and Methods

Cells and culture

C57BL/6 mouse-derived B16 melanoma cells (B16F10), human umbilical vein endothelial cells (HUVECs), and hepatocellular carcinoma (HCC) cell line BEL-4702 cells were purchased from American Type Culture Collection and cultured in Iscove's modified Dulbecco's medium (IMDM; Gibco®, Life Technologies) supplemented with 10% fetal bovine serum (FBS) (Invitrogen, Life Technologies) and penicillin–streptomycin antibiotics (Invitrogen) in an incubator (Heraeus) with 5% CO_2 at 37°C.

ODNs

The various lengths of ODNs focusing on the contiguous guanosines and CpG motif were rationally designed by our lab and synthesized by the TAKARA Biotech Company. All of these sequences are shown in Fig. 1. The sequences in the box represent phosphodiester linkage, and the sequences outside the box represent phosphorothioate linkage. The 2216 (5′-ggGGGACGATCGTCgggggG-3′), 2006 (5′-TCGTCGTTTTGT CGTTTTGTCGTT-3′) and C274 (5′-TCGTCGAACGTTCGA GATGAT-3′) were respectively used as well-known typical A-type, B-type, and C-type CpG ODNs controls (capital and lowercase letters respectively represent phosphorothioate and phosphodiester linkage). All ODNs were diluted in phosphate buffered saline (PBS) buffer (pH 7.0), and tested negative for detectable endotoxins via the Limulus amebocyte lysate assay (Associates of Cape Cod, Inc.).

Mice

All *in vivo* experiments were carried out using 6- to 8-week-old female C57BL/6 mice (Vital River). The experimental manipulation of the mice was undertaken in accordance with the National Institutes of Health *Guide for the Care and Use of Laboratory Animals*, with the approval of the Scientific Investigation Board of Science & Technology of Jilin Province.

Materials and instruments

A 96-well Costar® plate was used. Thiazolyl blue tetrazolium bromide (MTT) powder and dimethyl sulfoxide (DMSO) solution were purchased from Sigma-Aldrich. The Thermo Scientific Multiskan Ascent Microplate Reader (ThermoFisher Scientific) was used for the MTT assay.

In vitro *assay*

Cell adhesion in culture plate. A total of 4×10^4 cells per well in 100 μL of IMDM containing 10% FBS was seeded in a 96-well plate and co-cultured with ODN at 6 μg/mL or equal volume of PBS at 37°C incubator. Four replicate wells were used for each sample. After incubation for 40 minutes, nonadherent cells were slightly washed away with PBS and the remaining cells were digested and counted. The average number of four replicate wells was used to calculate the adhesion ratio of each ODN compared to PBS control.

Cell adhesion in fibronectin-coated plate. In one procedure, the 96-well culture plate was coated by fibronectin (FN) at 10 μg/mL and incubated at 37°C for 30 minutes, then washed by PBS three times, following which mixtures containing 4×10^4 B16 cells and BW001 at 6 μg/mL were added in each well. In another procedure, the 96-well culture plate was coated by a mixture containing fibronectin (FN) at 10 μg/mL and BW001 at 6 μg/mL and incubated at 37°C for 30 minutes, then washed by PBS three times, following which suspensions of 4×10^4 B16 cells were added in each well. After incubation, the plate was treated in the same way as mentioned above.

Cell adhesion in collagen type 1 coated plate. In one procedure, 25 μL of collagen (73 μg/mL) was added to 75 μL PBS in each well on ice and incubated at 37°C until collagen solidification, then mixtures of 4×10^4 B16 cells and BW001 at 6 μg/mL were added to each well. In another procedure, a 96-well culture plate was coated by the mixtures of collagen and BW001 at 6 μg/mL, following which suspensions of 4×10^4 B16 cells were added in each well. The plate was treated in the same way as mentioned above.

Cell adhesion to endothelial cells. A total of 4×10^4 HUVECs in 100 μL IMDM were seeded in the 96-well plate and cultured in a 37°C incubator overnight to form a confluent monolayer, then 4×10^4 tumor cell suspensions containing 6 μg/mL ODN were added into the HUVEC monolayer. The plate was treated in the same way as mentioned above.

Adhesion assay ex vivo

A 6- to 8-week-old female C57BL/6 mouse was sacrificed and the lungs were separated for the preparation of serial frozen sections at 6 microns. A suspension of PKH26-labeled B16 cell (4×10^4 cells in 50μL PBS) containing 6 μg/mL BW001 was dropped to the sections and co-cultured in a 37°C incubator for 40 minutes. Nonadherent cells were slightly washed away, and then the sections were fixed with 4% polyoxymethylene, and covered with 20% glycerol. The number of adherent cells was counted under fluorescence microscopy.

MTT assay

A suspension (100 μL) containing 4×10^4 B16 cells and 6 μg/mL ODN was cultured in the 96-well plate for 24 hours. Then 10 μL MTT (5 mg/mL) was added to each well and incubated in a light, tight container for an additional 4 hours at 37°C. DMSO in the amount of 150 μL was added to each well, and the plate was put into a shaker for 20 minutes to make a full solution of formazan; then, the optical density (OD) value

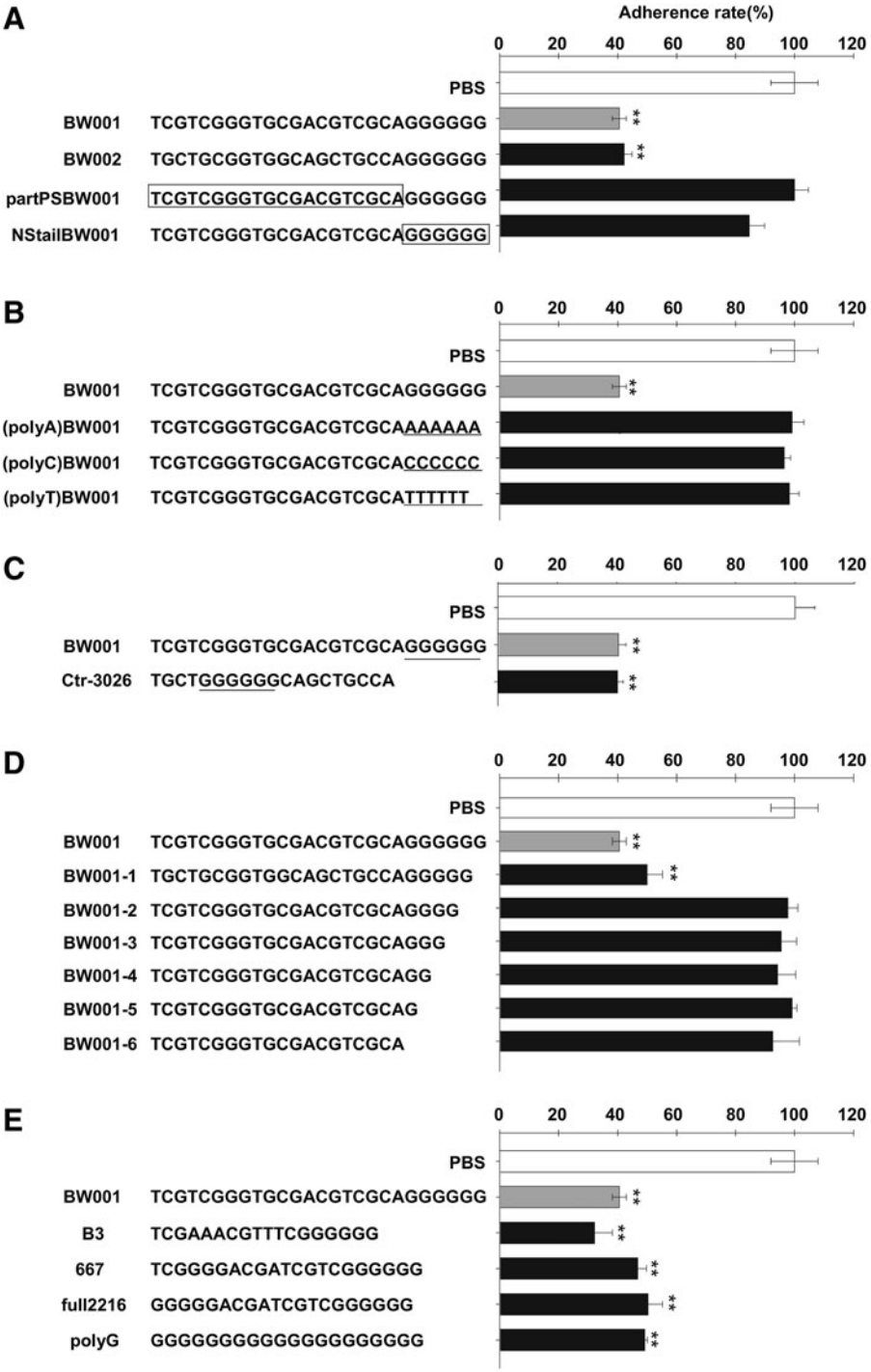

FIG. 1. The sequence features of BW001 on adhesion-inhibiting ability. B16 cells (4×10^4 per well) were co-cultured with ODN at 6μg/mL for 40 minutes at 37°C. Non-adherent cells were slightly washed away with PBS and the number of adherent cells in four replicate wells was counted. Results were expressed as adherence rate ± SD by columns. The average number of four replicate wells was used to calculate the adhesion ratio of each ODN compared to PBS control. **(A)** The influence of CG motif and phosphorothioate (PS) modification. BW002 was GC reversed form of BW001 partPSBW001 and NStailBW001 were partially PS-modified versions of BW001. The sequences in box were phosphodiester linkage, and the sequences outside the box were phosphorothioate linkage. **(B)** The influence of polyG tail. (polyA) BW001, (polyC) BW001, and (polyT) BW001 were the forms that replaced the ployG tail, with polyA, polyC, and polyT, respectively, at 3′ end as indicated with underline. **(C)** The influence of the position of polyG motif. The position of polyG motif is underlined. **(D)** The influence of the number of guanine bases in polyG tail. BW001-1 ~ BW001-6 are, respectively, the forms owning a gradually decreased numbers of guanine base in polyG tail. **(E)** The sequence-effect relationship of BW001-like ODN. The ODNs used were indicated in the figure. Three independent experiments were performed, and data from one representative experiment of three are shown. Unpaired 2-tailed Student's *t*-test was applied to analyze the data. $^{**}p<0.001$ versus PBS.

at A578 was read on the microplate reader. The viable cell numbers were calculated according to the standard curve (Wang et al., 2008; Sylvester, 2011).

Cell cycle analysis

B16 cells were harvested, and the cell concentration was adjusted to 1×106 cells/mL after being treated for 24 hours according to the procedure mentioned above for the MTT assay. The cell suspension was fixed with 75% pre-cooled alcohol and stained with propidium iodide (PI), and then the PI-labeled cells were analyzed using flow cytometry (Song et al., 2011).

In vivo *experiments*

The mice were randomly grouped for *in vivo* experiments. A total of 3.5×10^5 B16 cells were harvested in log-phase growth and rinsed three times with PBS, then resuspended in PBS and administered in a volume of 0.2 mL [in the intraperitoneal (i.p.) and subcutaneous (s.c.) models] or 0.1 mL [in the intravenous (i.v.) model] containing 25 μg ODN per mouse according to a different procedure.

In the i.p. model, the mice ($n=4$–5) were inoculated with tumor cells and sacrificed 7 days later. The number of colonies was counted in the peritoneal cavity of each mouse. In another

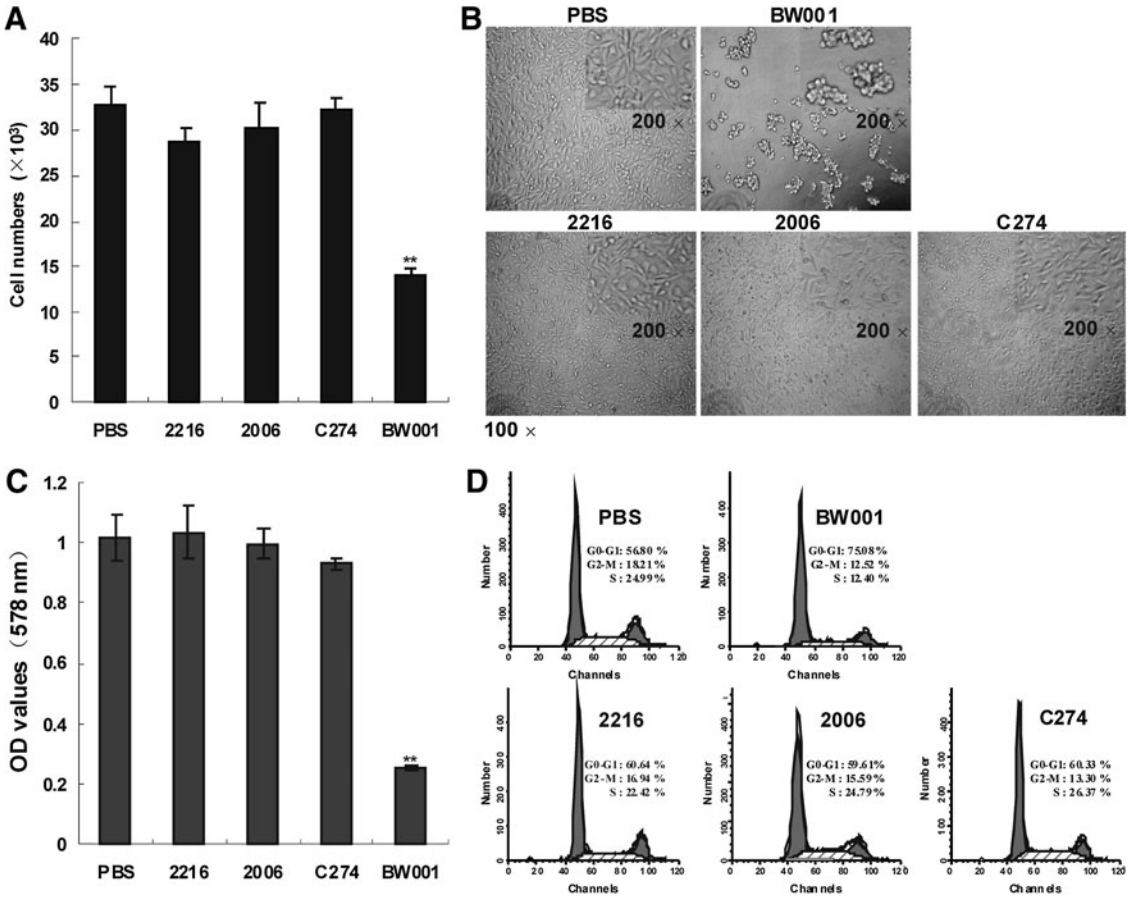

FIG. 2. Adhesion, spreading, and proliferation of BW001-treated melanoma cell. **(A)** Cell adhesion assay. B16 cells (4×10^4 per well) were co-cultured with oligodeoxynucleotides (ODN) at 6 μg/mL for 40 minutes at 37°C. Nonadherent cells were slightly washed away with phosphate buffered saline (PBS) and the number of adherent cells in four replicate wells was counted. Three independent experiments were performed, and data from one representative experiment of three are shown. Each column represents cell numbers ± standard deviation (SD). Unpaired 2-tailed Student's *t*-test was applied to analyze the data. $^{**}p<0.001$ versus others. **(B)** Cell spreading state. B16 cells were co-cultured with ODN at 6 μg/mL for 24 hours at 37°C and then photographed (100× magnification; upper right corner of each image shows 200× magnification). **(C)** Thiazolyl blue tetrazolium bromide (MTT) assays displayed the viable B16 cells in the CpG ODN-treated wells after co-culture for 24 hours. Four independent experiments were performed and data from one representative experiment are shown. Each column represents optical density (OD) values ± SD. Unpaired 2-tailed Student's *t*-test was applied to analyze the data. $^{**}p<0.001$ vs. others. **(D)** The propidium iodide (PI) nuclei staining and flow cytometry assay were accomplished as described in methods section. Numbers in each histogram indicate the cell percentage in the G1/G0, G2/M, and S phases of the cell cycle. Three independent experiments were performed, and data from one representative experiment of three are shown.

procedure, 10 mice in each group were monitored for 30 days after tumor challenge for recording their survival time.

In the s.c. model, the mice ($n=10$) were inoculated with tumor cells at the back near the right leg. Tumor diameter was measured with a caliper every other day beginning with the appearance of palpable nodes. The measurements were continued until one tumor-bearing mouse expired. Tumor volume was calculated as length × width^2 × 0.52.

In the i.v. model, the mice ($n=7$–10) were inoculated with tumor cells by lateral tail vein injection. All mice were sacrificed 21 days after tumor challenge, and lung tissue was separated for counting the number of tumor colonies.

Statistical analysis

Statistical analysis was performed using commercially available software (SPSS 13.0 for Windows™). Cell adhesion rates and cell proliferation were analyzed by the unpaired 2-tailed Student's *t*-test. Tumor colony number and tumor size were compared by nonparametric tests. Tumor growth rate was analyzed by a repeated-measure analysis of variance (one-way analysis of variance test). Survival curves were calculated by the Kaplan–Meier method, and differences between curves were evaluated by the log-rank test. A *p*-value of <0.05 was considered statistically significant.

Results

BW001-treated B16 cells displayed decreased adhesion, spreading, and proliferation ability

Recent studies have revealed that CpG-ODNs can affect immune cell adherence (Macfarlane et al., 1999; Sanjuan et al., 2006), but the effect of CpG ODN on tumor cell adhesion is still unclear. The B16 melanoma cell was used for this

purpose. We co-cultured B16 cells with a series of CpG ODN at 6 μg/mL for 40 minutes at 37°C, and found that a self-designed CpG ODN BW001 decreased the adherent numbers of B16 cells ($p < 0.001$ vs. PBS) to a plastic plate, while well-known CpG ODNs (CpG 2216, 2006, and C274) did not affect the adhesion of the B16 cells ($p > 0.05$ vs. PBS) (Fig. 2A). Moreover, the cells treated with BW001 clumped together compared with the spreading state of the cells in the 2216-, 2006- and C274-treated wells after further culture for another 12 hours (Fig. 2B). Simultaneously, the viable cell numbers determined by the MTT assay (Fig. 2C) and percentage of S-phase cells determined by flow cytometry (Fig. 2D) were the lowest in the BW001 wells after co-culturing for 24 hours ($p < 0.001$ vs. PBS or vs. the other CpG ODNs mentioned above), indicating that BW001 indirectly reduces the proliferation of B16 cells by inhibiting the cells' adhesion.

Full PS modification and the polyG motif were necessary for the adhesion-inhibiting activity of BW001

To explore the sequence features of BW001 on the inhibition of B16 cell adhesion, we synthesized a series of similar ODNs. First, we found that BW002, the guanine-cytosine (GC)-reversed form of BW001, had an effect similar to that of BW001 ($p > 0.05$) (Fig. 1A). But partPSBW001 or NStailBW001, respectively, representing the form of only the polyG tail to be phosphorothioated or the backbone to be phosphorothioated of BW001, could not inhibit the adhesion of B16 cells ($p > 0.05$ vs. PBS) (Fig. 1A). Furthermore, we replaced the polyG motif at the 3′ end of BW001 with polyA, polyC, or polyT, respectively, designated as (polyA)BW001, (polyC)BW001, and (polyT)BW001, which failed to inhibit the adhesion of B16 cells ($p > 0.05$ vs. PBS) (Fig. 1B). However, there was no influence on the anti-adhesive activity of the BW001 when the position of the polyG motif was changed from the 3′ end into the middle of the sequence (which was named Ctr-3026, $p < 0.001$ vs. PBS; $p > 0.05$ vs. BW001) (Fig. 1C). Then, we decreased a guanine base in the polyG tail of BW001 to form a new ODN named BW001-1 with 5 contiguous guanosines, which still possessed adhesion-inhibiting activity ($p < 0.001$ vs. PBS), rather than BW001-2 ~ BW001-6 with 4 or fewer than 4 guanosines ($p > 0.05$ vs. PBS) (Fig. 1D). Next, we tested the influence of a series of BW001-like ODNs with full-PS structure and the polyG motif on the adhesion activity of the B16 cells. As shown in Fig. 1E, all these BW001-like ODNs could inhibit adhesion of the B16 cells ($p < 0.001$ vs. PBS; $p > 0.05$ vs. BW001). The data show that the B16 cell adhesion-inhibiting activity of BW001 depends on the existence of a full-PS backbone and more than four contiguous guanosines, but in a CpG motif-independent manner.

BW001-treated B16 cells displayed decreased adhesion ability on a plate coated by FN or type 1 collagen

Both FN and collagen belong to the ECM and are advantageous for a malignant tumor's invasion and metastasis (Menter and Dubois, 2012; Neri and Bahlis, 2012). We therefore used FN and collagen type 1 to mimic the ECM and observe the influence of BW001 on the adhesion of B16 cells to the ECM. We found that the number of adherent B16 cells was less in the BW001 wells than in the PBS wells in the plate coated by FN (Fig. 3A) or type 1 collagen (Fig. 3B). Moreover, when B16 cells were added to the plate pre-coated by the mixture of BW001 with FN or type 1 collagen, the adhesion rate was reduced only in the wells coated by FN plus BW001 (Fig. 3C), rather than in the wells coated by collagen plus BW001 (Fig. 3D). However, we found that the gel formed by collagen type 1 was brittle and easy to break (data not shown). The results suggest that BW001 has the potential to inhibit the adhesion of B16 cells on ECM-like substrates.

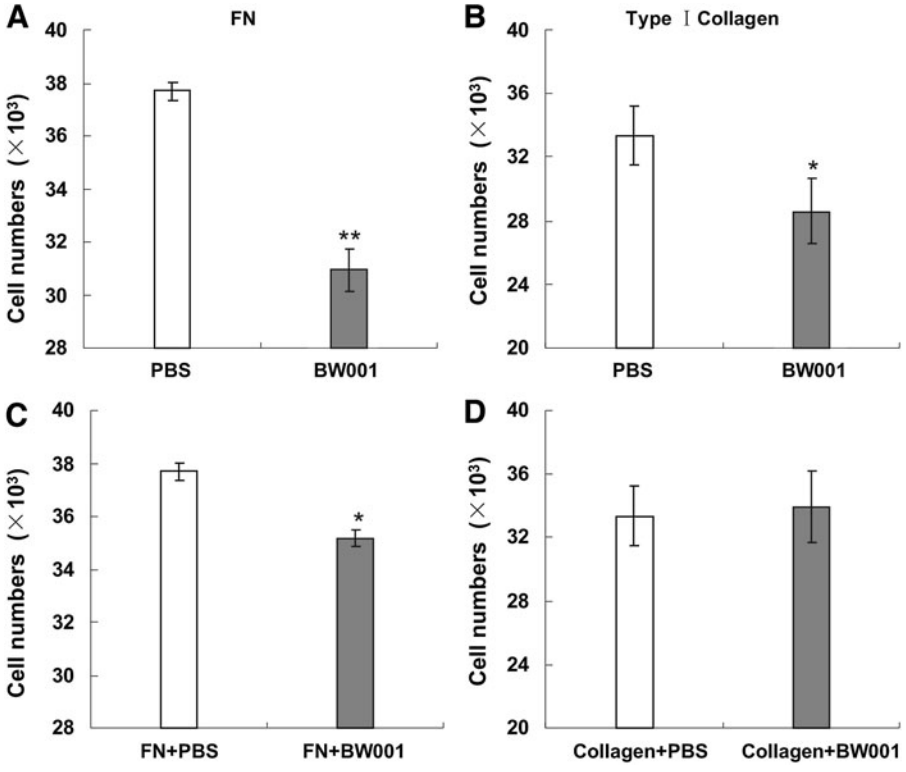

FIG. 3. The influence of BW001 on B16 cell adhesion ability in a plate coated by fibronectin (FN) or type 1 collagen. In one procedure, the 96-well plate was coated with FN at 10 μg/mL **(A)** or type 1 collagen at 18.25 μg/mL **(B)**. Suspensions of 4×10^4 B16 cells containing BW001 at 6μg/mL were added in each well and co-cultured for another 40 minutes. In another procedure, the 96-well culture plate was coated by a mixture containing FN at 10 μg/mL **(C)** or type 1 collagen at 18.25 μg/mL **(D)** with BW001 at 6 μg/mL and incubated at 37°C for 30 minutes, following which suspensions of 4×10^4 B16 cells were added in each well. Nonadherent cells were slightly washed away with PBS and the average number of adherent cells in four replicate wells was counted. Three independent experiments were performed, and data from one representative experiment of three are shown. Unpaired 2-tailed Student's *t*-test was applied to analyze the data. *$p < 0.05$ versus PBS; **$p < 0.001$ versus PBS.

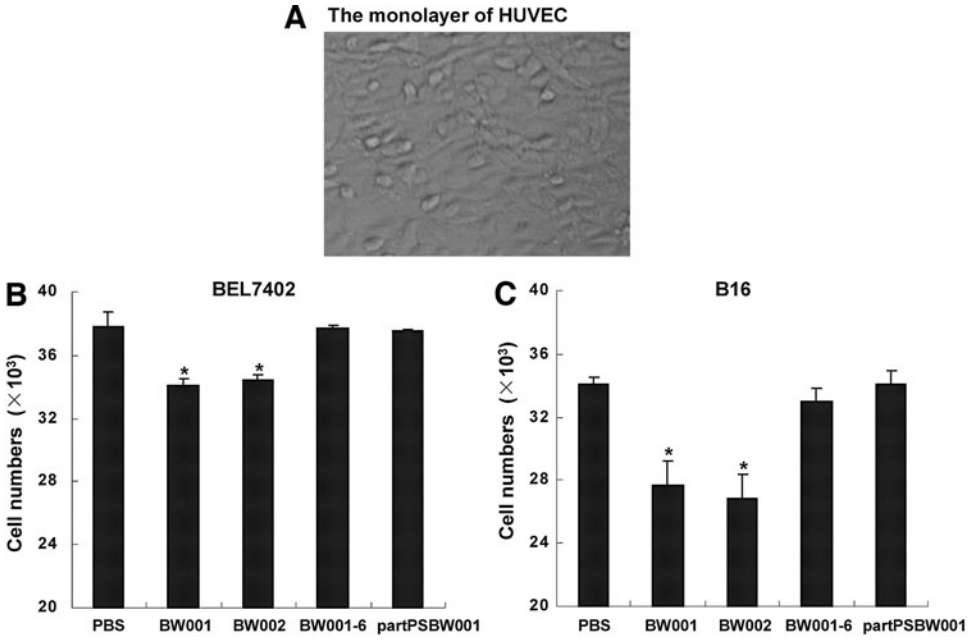

FIG. 4. The influence of BW001 on B16 cell adhesion to endothelial cells. A total of 4×10^4 human umbilical vein endothelial cells (HUVECs) in 100 μL Iscove's modified Dulbecco's medium were seeded in the 96-well plate and cultured in a 37°C incubator overnight to form a confluent monolayer **(A)**, then 4×10^4 BEL-7402 cell **(B)** or B16 cell **(C)** suspensions containing ODN at 6 μg/mL were added into the HUVEC monolayer and co-cultured at 37°C for 40 minutes. Nonadherent cells were slightly washed away with PBS and the average number of adherent cells was counted in 4 replicated wells. Three independent experiments were performed, and data from one representative experiment of three are shown. Unpaired 2-tailed Student's *t*-test was applied to analyze the data. $^*p<0.05$ versus PBS.

BW001-treated B16 cells displayed decreased adhesion to endothelial cells and lung tissue in vitro

The adhesion of tumor cells to endothelial cells is a critical step for tumor metastasis (Karmali et al., 2011; Braeuer et al., 2012). To observe the influence of BW001 on the adhesion of B16 cells to endothelial cells, we incubated a mixture of B16 cells with BW001 or control ODNs including BW002, partPSBW001, BW001-6 on monolayer HUVECs (Fig. 4A) for 40 minutes. HCC BEL-4702 cells were used as B16 cells'

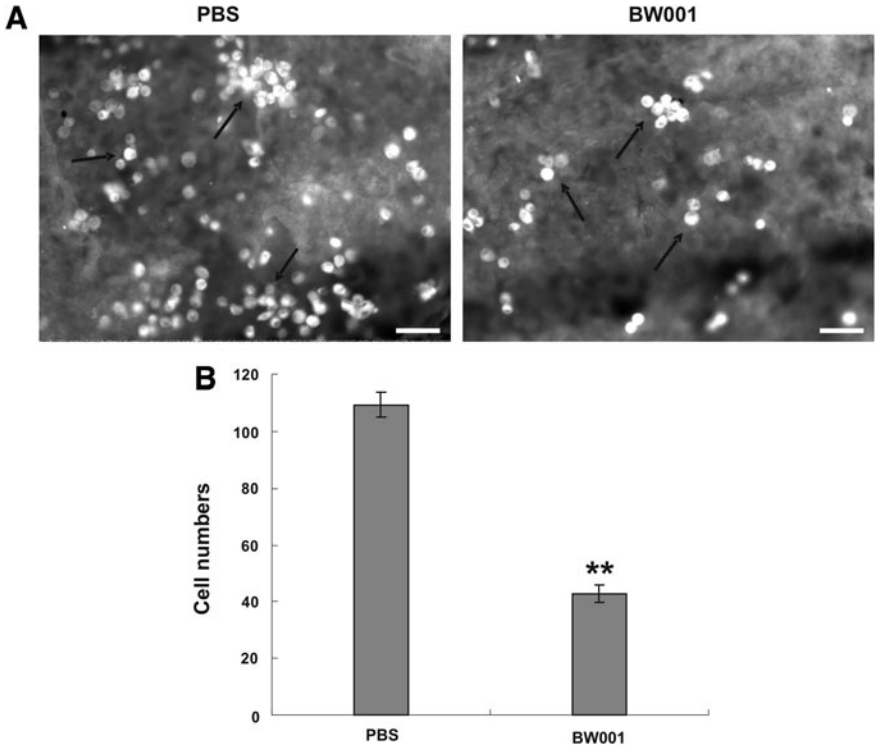

FIG. 5. The influence of BW001 on B16 cell adhesion to lung tissue. PKH26-labeled B16 cells suspensions containing BW001 at 6 μg/mL was incubated on fresh cryostat sections of lung tissue at 37°C for 40 minutes. Then, nonadherent cells were slightly washed away and adherent cells were fixed. **(A)** Representative lung tissue sections were photographed under fluorescence microscopy (magnification 200×, open bars = 6 μm). Adherent cells are indicated with arrows. **(B)** Adherent B16 cell numbers on lung tissue sections. Three independent experiments were performed, and data from one representative experiment of three are shown. Unpaired 2-tailed Student's *t*-test was applied to analyze the data. $^{**}p<0.001$ versus PBS.

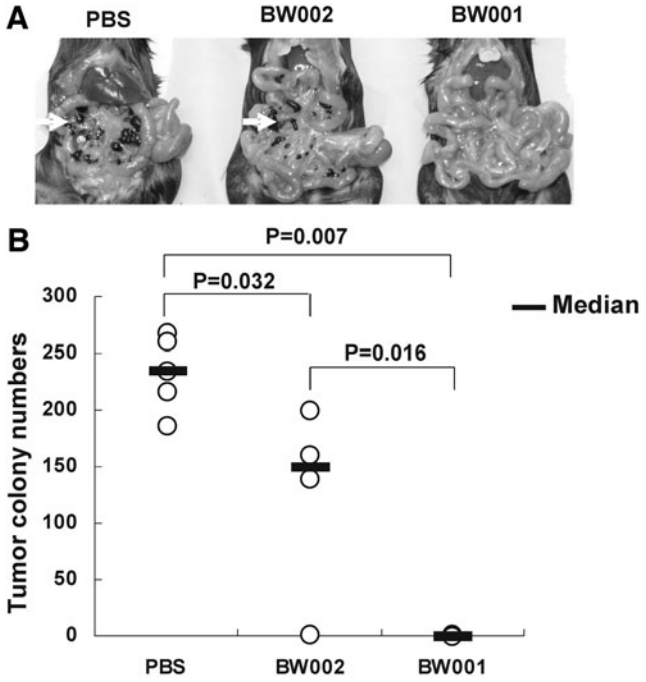

FIG. 6. Melanoma colony formation in mouse peritoneal cavity. Female C57BL/6 mice were intraperitoneally injected with 3.5×10^5 B16 cell suspensions containing indicated ODN (25 μg per mouse) or PBS. All mice were sacrificed 7 days later. **(A)** Representative melanoma colony formation in the peritoneal cavity of mice in each group was indicated. Open arrows indicate the melanoma colonies. **(B)** The melanoma colony numbers in the peritoneal cavity of mice. Each number is represented by an open circle ($n=4$–5).The geometric mean of each group is indicated by a horizontal bar. Statistical significance was determined using the nonparametric test; p values are shown between each group.

control. The results showed that the numbers of adherent BEL-4702 cells (Fig. 4B) or B16 cells (Fig. 4C) in both the BW001 and BW002 groups were less than in the PBS group ($p<0.05$); nevertheless, there were no differences between partPSBW001 or BW001-6 and the PBS group ($p>0.05$ vs. PBS). This indicated that a BW001-like structure can inhibit the adhesion of tumor cells to endothelial cells.

Melanoma easily disseminates to the lung, so the adhesion of melanoma cells to lung tissue is crucial for lung metastasis (Karmali et al., 2011). To identify the effect of BW001 on the adhesion of B16 cells to lung tissue, we incubated a mixture of PKH-26-stained B16 cells with BW001 on a fresh cryostat section of mouse lung tissue and calculated the number of adherent cells under the fluorescent microscope. As shown in Fig. 5, there were significantly fewer adherent cells in the BW001 group than in the PBS group ($p<0.001$), suggesting that BW001 can inhibit the adhesion of melanoma cells to lung tissue.

The number of melanoma colonies decreased in the peritoneal cavity and the survival time of tumor-bearing mice was prolonged by BW001 treatment

Colony formation is the basis for the growth of tumors *in vivo*. In order to observe whether BW001 could influence the colony formation of melanoma B16 cells in the mouse peritoneal cavity, we inoculated B16 cell suspensions containing BW001 or BW002 into the peritoneal cavity of C57BL/6 mice. Seven days later, all of the mice were sacrificed and the number of melanoma colonies in the peritoneal cavity was counted. As shown in Fig. 6A, tumor colonies were scarcely found in the mice of the BW001 group, but there were significant numbers of tumor colonies in PBS group. The mean number of colonies in the BW001 group was the least ($p=0.007$ vs. PBS; $p=0.016$ vs. BW002), followed by the number of colonies in the BW002 group ($p=0.032$ vs. PBS) (Fig. 6B), suggesting that a BW001-like structure can decrease melanoma colony formation in the mouse peritoneal cavity, and the effect can be enhanced by the existence of the CpG motif.

However, tumor colony formation ability is just one predictor of a tumor's malignancy. Survival is an important indirect index to reflect the malignancy of a tumor. Therefore, we wished to investigate whether BW001 could prolong the survival of melanoma-bearing mice. Since BW001 and BW002 had different effects on the formation of melanoma colonies in the peritoneal cavity of mice, we set more ODN controls, including partPSBW001, BW001-6, and polyG_{20}. The cumulative survival rates in all the groups are shown in Fig. 7A. The mean survival (number of days) of the melanoma-bearing mice in the BW001 group was the longest ($p<0.05$ vs. all of others), followed by the survival rates of the partPSBW001 and BW001-6 groups ($p<0.05$ vs. PBS). There were no differences in the survival times of the mice among the polyG_{20}, BW002, and PBS groups ($p>0.05$). These results indicate that

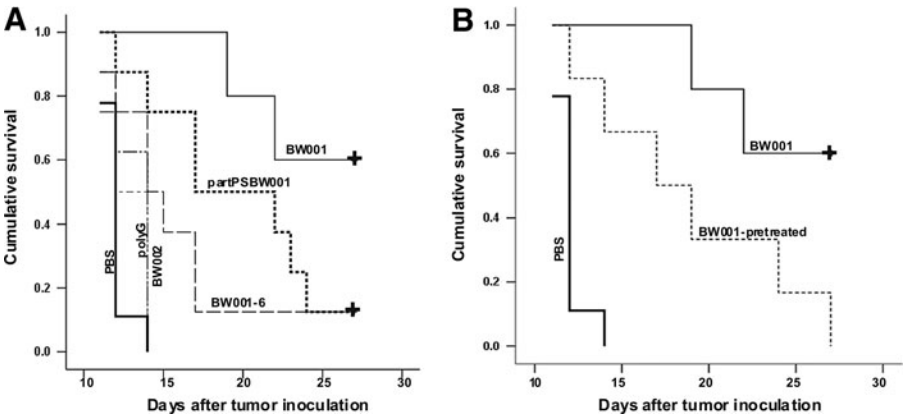

FIG. 7. The survival of melanoma-bearing mice. **(A)** Female C57BL/6 mice ($n=8$–10) were intraperitoneally inoculated with B16 cells (3.5×10^5/mouse) suspensions containing indicated ODNs (25 μg per mouse). **(B)** Female C57BL/6 mice ($n=6$–10) were intraperitoneally injected with BW001 (25 μg per mouse) 1 hour earlier before tumor challenge. Co-administration of 3.5×10^5 B16 cells and BW001 was used as control group. + represents censored data. Statistical significance was determined using the log rank test.

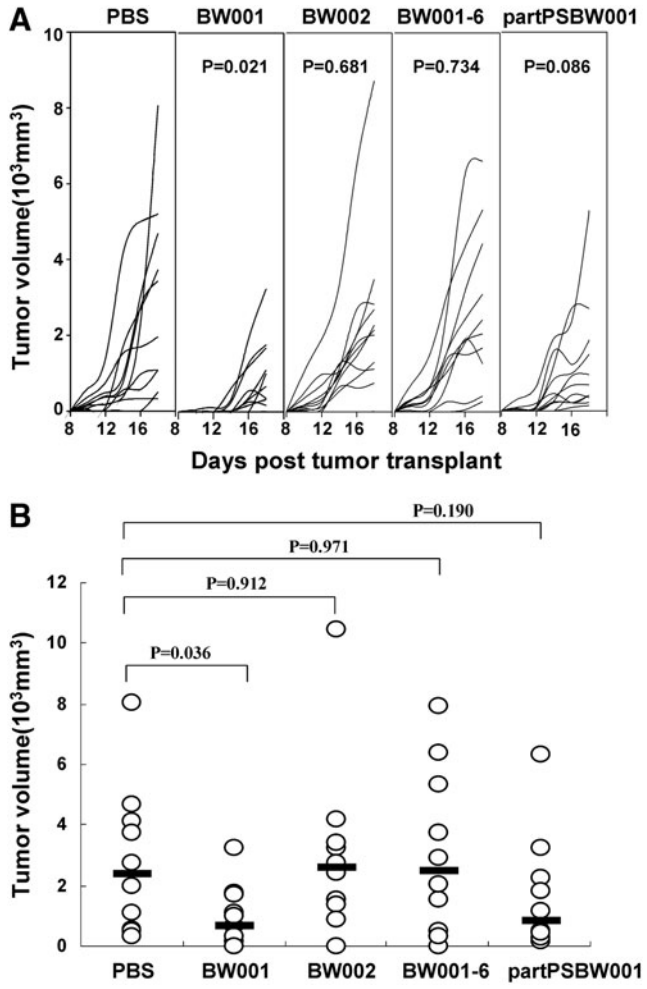

FIG. 8. The growth of subcutaneous melanoma. On day 0, female C57BL/6 mice were subcutaneously inoculated with 3.5×10^5 B16 cells suspensions containing ODN (25 μg per mouse). Tumor diameter was measured every other day beginning with the appearance of palpable nodes. Representative results from one of three independent experiments are shown. **(A)** Tumor growth curves. Each line represents an individual tumor growth curve in a single mouse. Statistical significance was analyzed by one-way ANOVA test; p values are shown between ODN and PBS. **(B)** Tumor volumes at the last measuring point. Each open circle denotes tumor size of a single mouse. The geometric mean of each group is indicated by a horizontal bar. Statistical significance was determined using the nonparametric test; p values are shown between ODN and PBS.

BW001 can prolong the survival of melanoma-bearing mice. This ability depends on the existence of the CpG motif and can be enhanced by the appearance of the polyG motif, suggesting that the antitumor effect of BW001 may be derived from multiple mechanisms.

Furthermore, we pre-injected BW001 i.p. 1 hour before tumor challenge; the co-administration of BW001 and B16 cells was applied as the control group. The cumulative survival of the mice in the BW001 pretreated group was prolonged compared with that of the PBS group ($p < 0.05$ vs. PBS), but it was still shorter than that of the BW001 and B16 cell co-administration group ($p < 0.05$) (Fig. 7B). This demonstrated that sufficient contact between BW001 and B16 cells plays an important role in the antitumor effect of BW001.

The growth of subcutaneous melanoma was delayed by BW001 treatment

To explore the effect of BW001 on tumor growth *in vivo*, the mice were subcutaneously inoculated with B16 cell suspensions containing BW001 or control ODNs including partPSBW001, BW001-6, BW002, and polyG20. The tumors were measured every 2 days beginning with the appearance of palpable nodes. Tumor growth curves and tumor volumes at the last measuring point of the individual animals are respectively presented in Figs. 8A and 8B. We found that tumor growth was arrested and tumor size was smaller in the BW001 group than in the PBS group ($p < 0.05$); however, there was no difference between that of other ODN groups and the PBS group ($p > 0.05$). The data suggest that BW001 can delay the growth of melanoma *in vivo*, and the effect depends on the coexistence of a full-PS backbone, and the CpG and polyG motifs.

Lung metastasis potential of B16 cells was reduced by BW001 treatment

Provided with the preceding results, we were eager to know whether BW001 could weaken the metastatic ability of melanoma. To answer this question, we injected B16 cell suspensions, which contained BW001 or control ODNs including partPSBW001, BW001-6, and BW002 into the lateral tail vein of mice. All the mice were sacrificed on day 21 after tumor challenge and the number of pulmonary metastatic melanoma colonies was determined. As shown in Fig. 9A, the number of melanoma colonies in the BW001 group was the lowest ($p < 0.001$ vs. all others), and the number of melanoma colonies in the other ODN groups were not different from the number in the PBS group ($p > 0.05$). Nevertheless, we found that there were no differences in colony numbers between the BW001 group and the other groups when BW001 was injected 1 hour before tumor challenge ($p > 0.05$) (Fig. 9B). This indicated that sufficient contact between BW001 and B16 cells is a necessary condition for the metastasis-inhibiting effect of BW001. However, in this experiment, we unfortunately found that 8 of 10 mice immediately died in the BW002 control group after injection of the mixture of B16 cells and the ODN, raising a new question which needs to be resolved by further research.

Discussion

Several years ago, Khaled et al. found that PS ODN with more than four contiguous guanosines could inhibit cell adhesion (Khaled et al., 1996). In the present study, we also found that self-designed ODN BW001, with the features mentioned above, was able to inhibit melanoma cell adhesion in various *in vitro* assays, and decreased the number of tumor colonies *in vivo* when the ODN was co-administered with the cells. Furthermore, the inclusion of a specific CpG motif endowed the ODN with the ability to inhibit melanoma growth and metastasis, suggesting that there are multiple mechanisms induced by BW001 in antitumor therapy.

The CpG motif is crucial for tumor growth inhibition *in vivo*. BW001 can inhibit the adhesion of melanoma *in vitro* and delay tumor growth *in vivo*; nevertheless, in the present

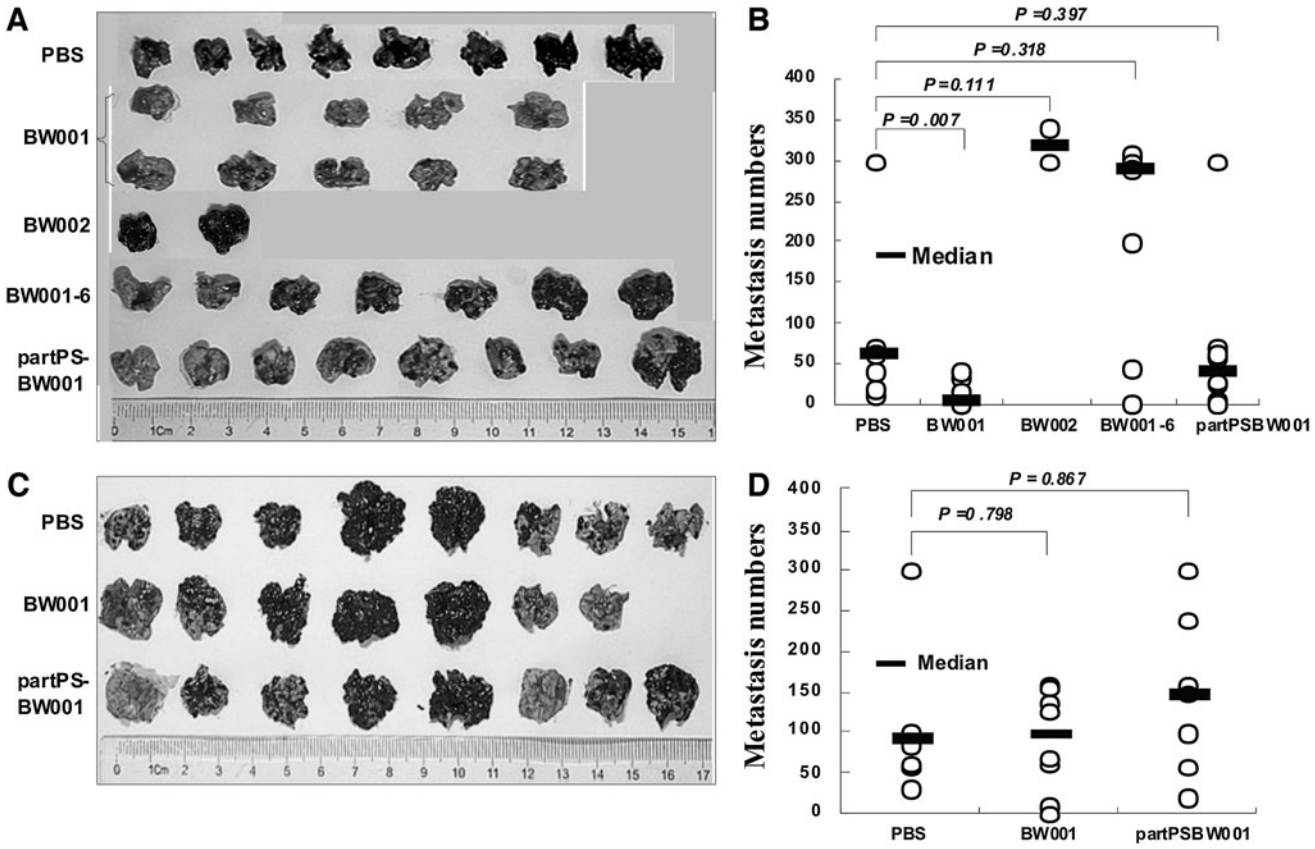

FIG. 9. Lung metastasis colony formation. **(A, B)** On day 0, suspensions of 3.5×10^5 B16 cells in a volume of 100 μL containing indicated ODN (25 μg per mouse) were injected into lateral tail veins of female C57BL/6 mice. On day 21, mice were sacrificed, lung tissues were separated **(A)** and the melanoma colony numbers on lung surface were counted **(B)**. **(C, D)** Female C57BL/6 mice were injected with BW001 (25 μg per mouse) into lateral tail vein 1 hour earlier than tumor challenge. Co-administration of tumor cell and ODN was used as control group. Lung tissue of each mouse was seperated **(C)** and melanoma colony numbers on lung surface were counted **(D)**. Colony numbers of each mouse are represented by open circles. The geometric mean of each group is indicated by a horizontal bar. Statistical significance was determined using the nonparametric test; *p* values are shown between ODN and PBS.

study, BW002 without the CpG motif only decreased colony formation of melanoma in the peritoneal cavity. These results are different from previously reported data that polyG is essential for the antitumor effect, but the CpG motif only augments the effect (Shen et al., 2002). Furthermore, BW001 still had an antitumor effect when being separately injected with tumor cells, even though the effect was weaker than that in the co-injection group in the i.p. model. However, it had no effect on the lung metastasis model, suggesting there are different mechanisms induced by BW001 to inhibit the growth of original and metastatic melanoma. Macrophages are abundant in the peritoneal cavity. CpG ODN can recognize TLR9 expressed in macrophages and stimulate tumor necrosis factor-alpha production by macrophages to indirectly induce an antitumor effect (Kuramoto et al., 2006). Suzuki et al. reported that TLR9-defective pulmonary alveoli macrophages had no reaction to CpG ODN (Suzuki et al., 2005), indicating that the effects of BW001 are possibly correlated with activation of the macrophages. In addition, paratumoral or intratumoral injection of CpG ODN can exert an integrated antitumor effect by stimulating activation of natural killer cells and CD8+ T cell (Auf et al., 2002; Lonsdorf et al., 2003), and inducing specific immune memory (Heckelsmiller et al., 2002). However, BW001, as an A-type CpG ODN, has a strong stimulation effect on the human immune system (Bao et al., 2006; Cong et al., 2007) but weak activation on the mouse immune system (data not shown), suggesting that BW001 might induce a stronger antitumor effect in the human counterpart melanoma model.

The inhibition effect of BW001 on original tumor growth and metastasis may be partially due to inhibition of the adhesion of tumor cells to the ECM or endothelial cells. GRO can inhibit tumor cell adhesion to the ECM and, as a result, inhibit tumor growth (Khaled et al., 1996; Saijo et al., 1997; Townsend et al., 2000). Blood vessels not only provide nutrition for tumor growth, but also supply the carrier for tumor metastasis (Zhu et al., 1992; Krishnan et al., 2005). In our study, we found that when BW001 was separately injected, it did not induce a metastasis-inhibiting effect similar to that of the BW001-B16 cells co-administered group, suggesting the possibility that contact of BW001 with melanoma cells may block the binding of melanoma cells with the metastasizing organ and therefore inhibit tumor metastasis.

The tumor-inhibiting effect of BW001 may partially benefit from the other antitumor properties of GRO except the inhibition of tumor cell adhesion. GRO can inhibit tumor cell proliferation (Dapić et al., 2002), delay the tumor cell cycle (Schwartz et al., 2008), exert cytotoxic effects (Goodchild et al.,

2007), and induce tumor cell apoptosis (Qi et al., 2006). All these effects are dependent on G-quadruplex formation (Dapić et al., 2003). In our study, BW001 with G-quartets could inhibit B16 cell adherence and decrease cell proliferation in an *in vitro* assay. The tumor growth-inhibiting activity of BW001 *in vivo* became weaker when the polyG tail was removed, further confirming the integrated antitumor effect of GRO. Based on these results, we will design more experiments to explore the other effects of BW001, for example, cytotoxicity other than an anti-adhesive effect on the inhibition of tumor growth *in vivo*.

Incidentally, BW002, BW001's GC-conversed form, seemed to be toxic when intravenously co-administered with B16 cells. We repeated the procedures three times, and found a similar phenomenon in which the mice immediately expired with co-administration of B16 cells and BW002. However, there was no such incident in the BW001 group (not all data shown), suggesting that the mixture of B16 cells and BW002 must form massive tumor pulmonary emboli and cause sudden death of mice (Chan et al., 2000). Therefore, it is possible that BW002 may more easily form intramolecular duplexes by itself or exist intermolecular interaction between BW002 and the surface molecular on B16 cells. This provides a new direction for further research.

In our study, we found an interesting phenomenon in that not only did the adhesion rate of BW001-treated melanoma cells decreased on a FN-pretreated culture plate, but also the adhesion rate of melanoma cells decreased on a FN + BW001-pretreated plate. Furthermore, we also observed that the gel formed by collagen type 1 was brittle and easier to break when BW001 was added to the collagen suspension (data not shown). This suggests the possibility that BW001 partially inhibits melanoma growth by hampering the formation of the ECM network. In addition, since both FN and collagen are important participatory components in abdominal adhesion, which is a common complication of surgery and chemotherapy (van Rijswijk et al., 1997; Uzunkoy et al., 2005), we suggest that BW001 might induce a comprehensive effect, including inhibiting melanoma reoccurrence and metastasis, while also reducing the formation of abdominal adhesions after surgery and chemotherapy.

In conclusion, we report that PS ODN with the polyG and CpG motifs can induce an integrated antitumor effect through multiple mechanisms other than inhibition of tumor cell adhesion. Additional research is needed to explore these mechanisms.

Author Disclosure Statement

No competing financing interests exist.

References

AUF, G., CHEN, L., FORNES, P., LE CLANCHE, C., DELATTRE, J.Y., and CARPENTIER, A.F. (2002). CpG-oligodeoxynucleotide rejection of a neuroblastoma in A/J mice does not induce a paraneoplastic disease. Neurosci. Lett. 327:189–192.

BAO, M., ZHANG, Y., WAN, M., DAI, L., HU, X., WU, X., WANG, L., DENG, P., WANG, J., CHEN, J., ET AL. (2006). CpG-induced tyrosine phosphorylation occurs via a TLR9-independent mechanism and is required for cytokine secretion. Clin. Immunol. 118:180–187.

BATES, P.J., LABER, D.A., MILLER, D.M., THOMAS, S.D., and TRENT, J.O. (2009). Discovery and development of the G-rich oligonucleotide AS1411 as a novel treatment for cancer. Exp. Mol. Pathol. 86:151–164.

BRAEUER, R.R., SHOSHAN, E., and KAMIYA, T. (2012). The sweet and bitter sides of galectins in melanoma progression. Pigment Cell Melanoma Res. 25:592–601.

CHAN, G.S., NG, W.K., NG, I.O., and DICKENS, P. (2000). Sudden death from massive pulmonary tumor embolism due to hepatocellular carcinoma. Forensic Sci. Int. 108:215–221.

CONG, Z., WAN, M., WU, X., WANG, L., HU, X., YANG, F., BAO, M., ZHANG, X., CHEN, J., WANG, L., and YU, Y. (2007). A CpG oligodeoxynucleotide inducing anti-coxsackie B3 virus activity in human peripheral blood mononuclear cells. FEMS Immunol. Med. Microbiol. 51:26–34.

DAMSKY, W.E., CURLEY, D.P., SANTHANAKRISHNAN, M., ROSENBAUM, L.E., PLATT, J.T., GOULD ROTHBERG, B.E., TAKETO, M.M., DANKORT, D., RIMM, D.L., MCMAHON, M., and BOSENBERG, M. (2011). β-catenin signaling controls metastasis in Braf-activated Pten-deficient melanomas. Cancer Cell 20:741–754.

DAPIć, V., ABDOMEROVIć, V., MARRINGTON, R., PEBERDY, J., RODGER, A., TRENT, J.O., and BATES, PJ. (2003). Biophysical and biological properties of quadruplex oligodeoxyribonucleotides. Nucleic Acids Res. 31:2097–2107.

DAPIć, V., BATES, P.J., TRENT, J.O., RODGER, A., THOMAS, S.D., and MILLER, D.M. (2002). Antiproliferative activity of G-quartet-forming oligonucleotides with backbone and sugar modifications. Biochemistry 41:3676–3685.

EL ANDALOUSSI, A., SONABEND, A.M., HAN, Y., and LESNIAK, M.S. (2006). Stimulation of TLR9 with CpG ODN enhances apoptosis of glioma and prolongs the survival of mice with experimental brain tumors. Glia 54:526–535.

GOODCHILD, A., KING, A., GOZAR, M.M., PASSIOURA, T., TUCKER, C., and RIVORY, L. (2007). Cytotoxic G-rich oligodeoxynucleotides: putative protein targets and required sequence motif. Nucleic Acids Res. 35:4562–4572.

HECKELSMILLER, K., RALL, K., BECK, S., SCHLAMP, A., SEIDERER, J., JAHRSDORFER, B., KRUG, A., ROTHENFUSSER, S., ENDRES, S., and HARTMANN, G. (2002). Peritumoral CpG DNA elicits a coordinated response of CD8 T cells and innate effectors to cure established tumors in a murine colon carcinoma model. J. Immunol. 169: 3892–3899.

KARMALI, P.P., BRUNQUELL, C., TRAM, H., IRELAND, S.K., RUOSLAHTI, E., and BILIRAN, H. (2011). Metastasis of tumor cells is enhanced by downregulation of Bit1. PLoS One 6:e23840.

KHALED, Z., BENIMETSKAYA, L., ZELTSER, R., KHAN, T., SHARMA, H.W., NARAYANAN R, and STEIN, C.A. (1996). Multiple mechanisms may contribute to the cellular anti-adhesive effects of phosphorothioate oligodeoxynucleotides. Nucleic Acids Res. 24: 737–745.

KIM, Y.H., GRATZINGER, D., HARRISON, C., BRODY, J.D., CZERWINSKI, D.K., AI, W.Z., MORALES, A., ABDULLA, F., XING, L., NAVI, D., ET AL ET AL. (2012). *In situ* vaccination against mycosis fungoides by intratumoral injection of a TLR9 agonist combined with radiation: a phase 1/2 study. Blood 119:355–363.

KRISHNAN, V., BANE, S.M., KAWLE, P.D., NARESH, K.N., and KALRAIYA, R.D. (2005). Altered melanoma cell surface glycosylation mediates organ specific adhesion and metastasis via lectin receptors on the lung vascular endothelium. Clin. Exp. Metastasis 22:11–24.

KURAMOTO, Y., NISHIKAWA, M., HYOUDOU, K., YAMASHITA, F., and HASHIDA, M. (2006). Inhibition of peritoneal

dissemination of tumor cells by single dosing of phosphodiester CpG oligonucleotide/cationic liposome complex. J. Control. Release 115:226–233.

LANGLEY, R.R., and FIDLER, I.J. (2007). Tumor cell-organ microenvironment interactions in the pathogenesis of cancer metastasis. Endocr. Rev. 28:297–321.

LI, H.Z., GAO, Y., ZHAO, X.L., LIU, Y.X., SUN, B.C., YANG, J., and YAO, Z. (2009). Effects of raf kinase inhibitor protein expression on metastasis and progression of human breast cancer. Mol. Cancer Res. 7:832–840.

LONSDORF, A.S., KUEKREK, H., STERN, B.V., BOEHM, B.O., LEHMANN, P.V., and TARY-LEHMANN, M. (2003). Intratumor CpG-oligodeoxynucleotide injection induces protective antitumor T cell immunity. J. Immunol. 171: 3941–3946.

MACFARLANE, D.E, and MANZEL, L. (1999). Immunos timulatory CpG-oligodeoxynucleotides induce a factor that inhibits macrophage adhesion. J. Lab. Clin. Med. 134:501–509.

MCGARY, E.C., HEIMBERGER, A., MILLS, L., WEBER, K., THOMAS, G.W., SHTIVELBAND, M., LEV, D.C., and BAR-ELI, M. (2003). A fully human antimelanoma cellular adhesion molecule/MUC18 antibody inhibits spontaneous pulmonary metastasis of osteosarcoma cells *in vivo*. Clin. Cancer Res. 9:6560–6566.

MENTER, D.G., and DUBOIS, R.N. (2012). Prostaglandins in cancer cell adhesion, migration, and invasion. Int. J. Cell Biol. 2012:723419.

NERI, P., and BAHLIS, N.J. (2012). Targeting of adhesion molecules as a therapeutic strategy in multiple myeloma. Curr. Cancer Drug Targets 12:776–796.

QI, H., LIN, C.P., FU, X., WOOD, L.M., LIU, A.A., TSAI, Y.C., CHEN, Y., BARBIERI, C.M., PILCH, D.S., and LIU, L.F. (2006). G-quadruplexes induce apoptosis in tumor cells. Cancer Res. 66:11808–11816.

SAIJO, Y., UCHIYAMA, B., ABE, T., SATOH, K., and NUKIWA, T. (1997). Contiguous four-guanosine sequence in c-myc antisense phosphorothioate oligonucleotides inhibits cell growth on human lung cancer cells: possible involvement of cell adhesion inhibition. Jpn. J. Cancer Res. 88:26–33.

SANJUAN, M.A., RAO, N., LAI, K.T., GU, Y., SUN ,S., FUCHS, A., FUNG-LEUNG, W.P., COLONNA, M., and KARLSSON, L. (2006). CpG-induced tyrosine phosphorylation occurs via a TLR9-independent mechanism and is required for cytokine secretion. J. Cell Biol. 172:1057–1068.

SCHWARTZ, T.R., VASTA, C.A., BAUER, T.L., PAREKH-OLMEDO, H., and KMIEC, E.B. (2008). G-rich oligonucleotides alter cell cycle progression and induce apoptosis specifically in OE19 esophageal tumor cells. Oligonucleotides 18:51–63.

SHEN, W., WALDSCHMIDT, M., ZHAO, X., RATLIFF, T., and KRIEG, A.M. (2002). Antitumor mechanisms of oligodeoxynucleotides with CpG and polyG motifs in murine prostate cancer cells: decrease of NF-kappaB and AP-1 binding activities and induction of apoptosis. Antisense Nucleic Acid Drug Dev. 2:155–164.

SOMMARIVA, M., DE CECCO, L., DE CESARE, M., SFONDRINI, L., MéNARD, S., MELANI, C., DELIA, D., ZAFFARONI, N., PRATESI, G., UVA, V., ET AL. (2011). TLR9 agonists oppositely modulate DNA repair genes in tumor versus immune cells and enhance chemotherapy effects. Cancer Res. 71:6382–6390.

SONG, X.J., YANG, C.Y., LIU, B., WEI, Q., KORKOR, M.T., LIU, J.Y., YANG, P. (2011). Atorvastatin inhibits myocardial cell apoptosis in a rat model with post-myocardial infarction heart failure by downregulating ER stress response. Int. J. Med. Sci. 8:564–572.

SUZUKI, K., SUDA, T., NAITO, T., IDE, K., CHIDA, K., and NAKAMURA, H. (2005). Impaired toll-like receptor 9 expression in alveolar macrophages with no sensitivity to CpG DNA. Am. J. Respir. Crit. Care Med. 171:707–713.

SYLVESTER, P.W. (2011). Optimization of the tetrazolium dye (MTT) colorimetric assay for cellular growth and viability. Methods Mol. Biol. 716:157–168.

TOWNSEND, P.A., VILLANOVA, I., UHLMANN, E., PEYMAN, A., KNOLLE, J., BARON, R., TETI, A., and HORTON, M.A. (2000). An antisense oligonucleotide targeting the alphaV integrin gene inhibits adhesion and induces apoptosis in breast cancer cells. Eur. J. Cancer 36:397–409.

UZUNKOY, A., BOLUKBAS, C., HOROZ, M., BOLUKBAS, F.F., and KOCYIGIT, A. (2005). The optimal starting time of postoperative intraperitoneal mitomycin-C therapy with preserved intestinal wound healing. BMC Cancer 5:31.

VAID, M., PRASAD, R., SUN, Q., and KATIYAR, S.K. (2011). Silymarin targets β-catenin signaling in blocking migration/invasion of human melanoma cells. PLoS One 6, e23000.

VAN RIJSWIJK, R.E., HOEKMAN, K., BURGER, C.W., VERHEIJEN, R.H., and VERMORKEN, J.B. (1997). Experience with intraperitoneal cisplatin and etoposide and i.v. sodium thiosulphate protection in ovarian cancer patients with either pathologically complete response or minimal residual disease. Ann. Oncol. 8:1235–1241.

WANG, X.J., LIU, J., WAN, M., WANG, L., WU, X.L., WEI, H.F., YU, Y.L., and WANG, L.Y. (2008). [Determination of optimized MTT colorimetric assay as the identification method for the activity of B type CpG ODN BW006]. Xi Bao Yu Fen Zi Mian Yi Xue Za Zhi. 24:69–71. [In Chinese]

WICKLEIN, D. (2012). RNAi technology to block the expression of molecules relevant to metastasis: the cell adhesion molecule CEACAM1 as an instructive example. Methods Mol. Biol. 878:241–250.

YAN, Y., CAO, Z., YANG, M., LI, H., WEI, H., FU, Y., SONG, D., WANG, L., and YU, Y.. (2012). A CpG oligodeoxynucleotide potentiates the anti-tumor effect of HSP65-Her2 fusion protein against Her2 positive B16 melanoma in mice. Int. Immunopharmacol. 12:402–407.

YANG, L., SUN, L., WU, X., WANG, L., WEI, H., WAN, M., ZHANG, P., YU, Y., and WANG, L. (2009). Therapeutic injection of C-class CpG ODN in draining lymph node area induces potent activation of immune cells and rejection of established breast cancer in mice. Clin. Immunol. 131:426–437.

ZENT, C.S., SMITH, B.J., BALLAS, Z.K., WOOLDRIDGE, J.E., LINK, B.K., CALL, T.G., SHANAFELT, T.D., BOWEN, D.A., KAY, N.E., WITZIG, T.E., and WEINER, G.J. (2012). Phase 1 clinical trial of CpG oligonucleotide 7909 (PF-03512676) in patients with previously treated chronic lymphocytic leukemia. Leuk. Lymphoma 53:211–217.

ZHU, D., CHENG, C.F., and PAULI, B.U. (1992). Blocking of lung endothelial cell adhesion molecule-1 (Lu-ECAM-1) inhibits murine melanoma lung metastasis. J. Clin. Invest. 89:1718–1724.

Address correspondence to:
Prof. Liping Wang
Department of Pathology
The Third hospital of Jilin University
126 Xiantai Street
Changchun, Jilin 130033
China

E-mail: xueju@mail.jlu.edu.cn

Received for publication January 26, 2013; accepted after review May 30, 2013.